FORCED CONVECTIVE FLOW OVER A POROUS PLATE WITH VARIABLE FLUID PROPERTIES AND CHEMICAL REACTION: AN APPLICATION OF THE LIE GROUP TRANSFORMATION

Kalidas Das[1], Nilangshu Acharya[2], and Pinaki Ranjan Duari[3]

[1]*Department of Mathematics, A.B.N.Seal College, Cooch Behar, W.B., India*
E-mail: kd.kgec@gmail.com
[2]*Depatment of Mathematics, P.R. Thakur Govt. College, Gaighata, Pin-743287, W.B., India*
E-mail: nilangshu.math@gmail.com
[3]*Department of Mathematics, Asansol Engineering College, Asansol, PIN-713305, India*
E-mail: pinakiranjanduari@gmail.com

(Received October 26, 2016)

Abstract

A study has been carried out to obtain solutions for heat and mass transfer in a forced magnetohydrodynamic convective flow of an electrically conducting incompressible fluid over a permeable flat plate embedded in a porous medium with thermal convective surface boundary conditions due to thermal radiation, temperature dependent viscosity, and thermal conductivity taking into account the first-order homogeneous chemical reaction. A scaling group of transformations has been applied to the governing equations. The transformed self-similar nonlinear ordinary differential equations, along with the boundary conditions, have been solved numerically using a fourth-order Runge–Kutta method and a Shooting technique. The effect of various relevant parameters on the flow field, temperature, concentration, wall skin friction, heat flux, and wall mass flux has been elucidated through graphs and tables. A comparison with previously published results has been presented.

1. Introduction

The group theory method is a classical method for finding similarity reduction of nonlinear differential equations. Similarity analysis reduces the number of variables that govern partial differential equations and consequently transforms it to ordinary differential equations. The Lie group transformation, which is a special form of the group method, is the most powerful and efficient method to provide similarity transforms; it is widely used in a nonlinear dynamical system. In the case of the scaling group of transformations, the group invariant solutions of initial and boundary value problems are nothing but well-known similarity solutions. The Lie group techniques have been applied by many researchers [1–7] to study different flow phenomena over different geometrics arising in fluid dynamics, plasma physics, aerodynamics, and other branches of engineering.

Convective flows in a porous media have been extensively studied in recent years due to wide applications in engineering, such as post-accidental heat removal in nuclear reactors, underground disposal of nuclear waste, solar collectors, drying processes, heat exchangers, geothermal and petroleum reservoir operations, building construction, etc. The stagnation flow problem was studied by Hiemenz [8], who developed an exact solution for the Navier–Stokes equations in a forced convective regime. Some authors considered various aspects of this problem and obtained similarity solutions (Tsai and Huang [9], Aziz [10] and Abdel-Rahman [11]). The governing equations of a fluid flow in a porous medium are nonlinear and difficult to handle analytically. Consequently, problems concerning flows in a porous medium are usually solved by numerical methods (Chamkha and Abdul-Rahim [12] and Seddeek et al. [13]). On the other hand, it is now well known that the classical Lie symmetry method can be systematically used to find similarity solutions, invariants, integrals motion, etc.; the usefulness of this approach is vividly illustrated by some authors in different contexts, namely, Pakdemirli and Yurusoy [14], Yurusoy and Pakdemirli [15] and Oberlack [16].

Many physical properties of materials, such as the phase, density, solubility, vapor pressure, and electrical conductivity, depend on temperature if the temperature gradient is high. In addition, the inertial, dispersion, thermal radiation, and suction/injection effects have a significant contribution to convective transport in a porous medium. Obviously, the combined effect of these parameters will have a large impact on heat and mass transfer rates. For lubricating fluids, the heat generated by the internal friction and the respective rise in temperature affect the fluid viscosity; therefore, the fluid viscosity can no longer be assumed to be a constant. An increase in temperature leads to a local increase in the heat transfer rate at the wall. Therefore, to predict the flow behavior correctly, it is essential to take into account the viscosity variation for incompressible fluids. Seddeek and Salem [17] studied a mixed convection flow with variable viscosity and variable thermal diffusivity. Kandasamy and Muhaimin [18] investigated the effect of temperature-dependent fluid viscosity on a magnetohydrodynamic free convective flow over a stretching surface using scaling transformations. The effect of variable fluid viscosity on the flow over a heated stretching sheet embedded in a porous medium was studied by Mukhopadhyay and Layek [19]. Hamad et al. [20] examined the effects of various physical parameters using the group method. Rahman and Eltayeb [21] discussed the convective slip flow of rarefied fluids over a wedge with a thermal jump and variable transport properties.

Studies of heat and mass transfer problems with chemical reaction are important in the chemical and hydrometallurgical industries; therefore, recently these studies have received a considerable amount of attention. A large number of research works was reported in this field. The effect of chemical reaction on a free convective flow under various flow configurations were studied by Patil and Kulkarni [22], Kandasamy et al. [23], Kandasamy et al. [24], Kandasamy et al. [25] and Yazdi et al. [26]. In the present study, the work of Hamad et al. [20] has been extended to investigate the effects of chemical reaction on a magnetohydrodynamic forced convective flow over a heated permeable flat plate embedded in a porous medium with variable fluid properties.

2. Mathematical Formulation of the Problem

2.1. Flow analysis

The case under study is a steady laminar coupled heat and mass transfer of an incompressible electrically conducting fluid over a permeable flat plate embedded in a porous medium in the presence of thermal radiation. The x and y-axes are taken along and perpendicular to the plate; the flow is assumed to be confined to $y \geq 0$ (Fig. 1). A uniform transverse magnetic field of strength B_0 is applied parallel to the y-axis. The bottom surface of the plate is heated by convection from a hot fluid of temperature T_f and this generates heat transfer coefficient h_f. The magnetic Reynolds number of the flow is taken to be small enough so that the induced magnetic field is assumed to be negligible in comparison with the applied magnetic field. The chemical reaction takes place in the flow; the viscous dissipation effect and the joule heat are neglected as the fluid is finitely conducting. The present case is limited to flows where the nonlinear Forchheimer term is neglected, while the linear Darcy term describing the distributed body force exerted by the porous medium is retained.

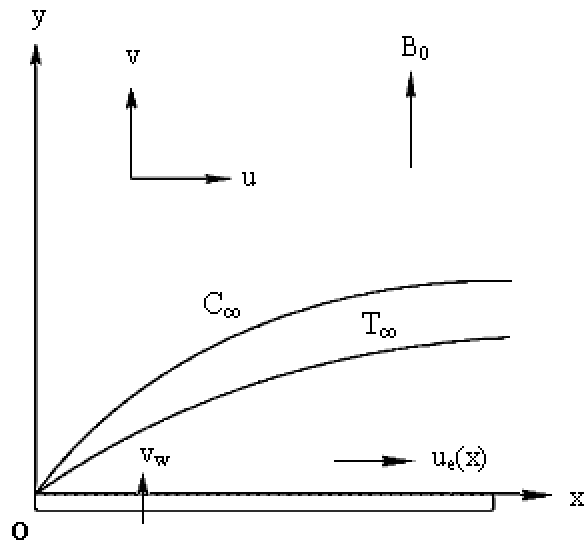

Fig. 1. Physical model and coordinate system of the problem.

Under the foregoing assumptions, the governing equations of this type of flow can be written as follows (Hamad et al. [20]; Kays and Crawford [27]):

$$\frac{\partial u}{\partial x}+\frac{\partial v}{\partial y}=0 \tag{1}$$

$$u\frac{\partial u}{\partial x}+v\frac{\partial u}{\partial y}=u_e\frac{du_e}{dx}+\nu\frac{\partial^2 u}{\partial y^2}+\frac{1}{\rho}\frac{\partial \mu}{\partial T}\frac{\partial T}{\partial y}\frac{\partial u}{\partial y}-\frac{\nu}{k}(\mathrm{u}-\mathrm{u}_e)-\frac{\sigma B_0^2}{\rho}(\mathrm{u}-\mathrm{u}_e) \tag{2}$$

$$u\frac{\partial T}{\partial x}+v\frac{\partial T}{\partial y}=\frac{1}{\rho c_p}\frac{\partial}{\partial y}\left(\kappa\frac{\partial T}{\partial y}\right)-\frac{1}{\rho c_p}\frac{\partial q_r}{\partial y} \tag{3}$$

$$u\frac{\partial C}{\partial x}+v\frac{\partial C}{\partial y}=D_m\frac{\partial^2 C}{\partial y^2}-k_r\left(C-C_\infty\right) \tag{4}$$

where u and v are the velocity components along the x- and y-axis respectively, u_e (x) is the stagnation point velocity in the viscid free stream, k is the permeability of the porous medium, ν is the kinematic viscosity, σ is the electrical conductivity, ρ is the fluid density, T is the temperature, C is the species concentration, c_p is the specific heat at constant pressure p, κ is thermal conductivity, q_r is the radioactive heat flux term, D_m is the mass diffusivity of species in fluid, and k_r is the rate of chemical reaction, where $k_r > 0$ represents destructive reaction, $k_r < 0$ represents generative reaction, and k_r =0 represents no reaction.

It is assumed that the bottom surface of the plate is heated by convection from a hot fluid at temperature T_f which provides heat transfer coefficient h_f. The boundary conditions at the plate surface and deep into the cold fluid can be written as follows (see Aziz [10]):

$$\left.\begin{aligned} &u = 0, v = v_w, C = C_w, -\kappa\frac{\partial T}{\partial y} = h_f\left(T_f - T_w\right) \text{ for } y=0 \\ &u \to u_e(x), T \to T_\infty, C \to C_\infty \text{ as } y \to \infty \end{aligned}\right\} \tag{5}$$

where v_w is the wall velocity. The fluid viscosity in the momentum boundary layer decreases with an increase in temperature, which, in turn, affects the heat transfer rate at the surface of the plate. Thus, to accurately predict the flow and heat transfer rates, Seddeek and Salem [17] suggested a temperature dependent viscosity in the form

$$\mu = \mu_\infty\left[a + b\left(T_\infty - T\right)\right] \tag{6}$$

where *a* and *b* are constants with *b* > 0, T_∞ is the temperature of the fluid outside the boundary layer, and μ_∞ is the dynamic viscosity at ambient temperature. Savvas et al. [29] observed that for liquid metals; the thermal conductivity varies linearly with temperature in a range of 0–400°F. Following Chiam [28] and Savvas et al. [29], the specific model for variable thermal conductivity is considered as

$$\kappa = \kappa_\infty\left(1 + c\frac{T - T_\infty}{\Delta T}\right) \tag{7}$$

where *c* is a constant which depends on the fluid and $\Delta T = T_w - T_\infty$. In the Rosseland approximation, radiative heat flux term q_r is given by

$$q_r = -\frac{4\sigma^*}{3k^*}\frac{\partial T^4}{\partial y} \tag{8}$$

where σ^* is the Stefan-Boltzmann constant and k^* is the mean absorption coefficient. Assuming that the differences in temperature within the flow are such that T^4 can be expressed as a linear combination of the temperature, T^4 is expanded in Taylor's series about T_∞ and neglecting the higher order terms, we have

$$T^4 = 4T_\infty^3 T - 3T_\infty^4 \tag{9}$$

Using Eqs. (8) and (9) in Eq. (3), we obtain

$$u\frac{\partial T}{\partial x}+v\frac{\partial T}{\partial y}=\frac{1}{\rho c_p}\frac{\partial}{\partial y}\left[\left(\kappa+\frac{16T_\infty^3\sigma^*}{3k^*}\right)\frac{\partial T}{\partial y}\right] \tag{10}$$

2.2. Non-dimensionalization of the governing equations

The following non-dimensional variables are introduced to convert the governing equations into a nondimensional form:

$$\left.\begin{array}{l} x'=\dfrac{x}{L},\, y'=\dfrac{y\sqrt{\mathrm{Re}}}{L},\mathrm{u}'=\dfrac{u}{U_\infty},v'=\dfrac{v\sqrt{\mathrm{Re}}}{U_\infty}, \\ u_e'=\dfrac{u_e}{U_\infty},\theta=\dfrac{T-T_\infty}{T_f-T_\infty},\phi=\dfrac{C-C_\infty}{C_w-C_\infty} \end{array}\right\} \tag{11}$$

where L is the characteristic length, U_∞ is the reference velocity, and $\mathrm{Re}=\frac{U_\infty L}{\nu}$ is the Reynolds number.

In addition, stream function ψ is defined by $u=\frac{\partial\psi}{\partial y},v=-\frac{\partial\psi}{\partial x}$. Thus, the equation of continuity (1) is satisfied automatically. Thus, relationships (6) and (7) become $\mu=\mu_\infty\left[1+\zeta(1-\theta)\right]$ and $\kappa=\kappa_\infty(1+\varepsilon\theta)$ respectively, where $\zeta=b\left(T_f-T_\infty\right)$ is the viscosity parameter and $\varepsilon=c\left(T_f-T_\infty\right)$ is the thermal conductivity parameter.

Using (11), the system of Eqs. (2), (4), and (10) becomes (dropping primes)

$$\frac{\partial\psi}{\partial y}\frac{\partial^2\psi}{\partial x\partial y}-\frac{\partial\psi}{\partial x}\frac{\partial^2\psi}{\partial y^2}=u_e\frac{du_e}{dx}+\left[1+\zeta(1-\theta)\right]\frac{\partial^3\psi}{\partial y^3}-\zeta\frac{\partial^2\psi}{\partial y^2}\frac{\partial\theta}{\partial y}-\left[M^2+\frac{1+\zeta(1-\theta)}{K}\right]\left(\frac{\partial\psi}{\partial y}-u_e\right) \tag{12}$$

$$\frac{\partial\psi}{\partial y}\frac{\partial\theta}{\partial x}-\frac{\partial\psi}{\partial x}\frac{\partial\theta}{\partial y}=\frac{1}{Pr}\left(1+\varepsilon\theta+\frac{4R}{3}\right)\frac{\partial^2\theta}{\partial y^2}+\frac{\varepsilon}{Pr}\left(\frac{\partial\theta}{\partial y}\right)^2 \tag{13}$$

$$\frac{\partial\psi}{\partial y}\frac{\partial\phi}{\partial x}-\frac{\partial\psi}{\partial x}\frac{\partial\phi}{\partial y}=\frac{1}{Sc}\frac{\partial^2\phi}{\partial y^2}-Kr\phi \tag{14}$$

and the boundary conditions turn into

$$\left.\begin{array}{l}\dfrac{\partial\psi}{\partial y}=0,\dfrac{\partial\psi}{\partial x}=f_w,\dfrac{\partial\theta}{\partial y}=\dfrac{1}{\lambda}\dfrac{1-\theta(0)}{1+\varepsilon\theta(0)},\phi=1 \text{ at } \ y=0\\ \dfrac{\partial\psi}{\partial y}\to x,\theta\to 0,\phi\to 0 \quad \text{as } \ y=0\end{array}\right\} \tag{15}$$

where Pr = $\frac{\mu_\infty c_p}{\kappa_\infty}$ is the Prandtl number, Sc = $\frac{\nu}{D_m}$ is the Schmidt number, $f_w=\frac{v_w}{U_\infty\sqrt{\text{Re}}}$ is the suction parameter, $\lambda=\frac{\kappa_\infty\sqrt{\text{Re}}}{Lh_f}$ is the surface convection parameter, $Kr=\frac{k_rL}{U_\infty}$ is the chemical reaction parameter, $K=\frac{\nu L}{kU_\infty}$ is the permeability parameter of the porous medium , $R=\frac{4T_\infty^3\sigma^*}{\kappa k^*}$ is the radiation parameter and $M=B_0\sqrt{\frac{\sigma L}{\rho U_\infty}}$ is the magnetic field parameter.

2.3. Lie symmetry groups and similarity solutions

The simplified form of Lie group transformations, namely, the scaling group of transformations is introduced as below

$$\Gamma: x^*=xe^{\varepsilon\alpha_1}, \text{y}^*=ye^{\varepsilon\alpha_2}, \psi^*=\psi e^{\varepsilon\alpha_3},\ \theta^*=\theta e^{\varepsilon\alpha_4}, \phi^*=\phi e^{\varepsilon\alpha_5} \tag{16}$$

Here, ε is the parameter of the group and α'S are arbitrary real numbers whose interrelationship will be determined by the present analysis. Equation (16) can be considered as a point-transformation, which transforms coordinates (x, y,ψ, θ,ϕ) to coordinates $\left(x^*,\ \text{y}^*,\ \psi^*,\ \theta^*,\ \phi^*\right)$. Substituting (16) in (12)–(14), the following relationships of the exponents are obtained:

$$\left.\begin{array}{l}\alpha_1+2\alpha_2-2\alpha_3=3\alpha_2-\alpha_3-\alpha_4=3\alpha_2-\alpha_3=\alpha_2-\alpha_3=\alpha_2-\alpha_3-\alpha_4;\\ \alpha_1+\alpha_2-\alpha_3-\alpha_4=2\alpha_2-\alpha_4=\alpha_2-\alpha_4;\\ \alpha_1+\alpha_2-\alpha_3-\alpha_5=2\alpha_2-\alpha_5=-\alpha_5\end{array}\right\} \tag{17}$$

These relations give $\alpha_1=\alpha_3,\alpha_2=\alpha_4=\alpha_5=0$. Thus, the set of transformations (16) reduces to a one parameter group of transformation:

$$\Gamma: x^*=xe^{\varepsilon\alpha_1}, \text{y}^*=y, \psi^*=\psi e^{\varepsilon\alpha_1}, \theta^*=\theta, \phi^*=\phi \tag{18}$$

Expanding by the Taylor's method in powers of ε and keeping terms up to the order of ε, we obtain

$$x^* - x = x\varepsilon\alpha_1, y^* - y = 0, \psi^* - \psi = \psi\varepsilon\alpha_1, \theta^* - \theta = 0, \phi^* - \phi = 0 \tag{19}$$

These relationships lead to the following characteristic equations for similarity:

$$\frac{dx}{x} = \frac{dy}{0} = \frac{d\psi}{\psi} = \frac{d\theta}{0} = \frac{d\phi}{0} \tag{20}$$

from which the similarity variables, velocity, temperature, and concentration are found to have the following form:

$$\eta = y, \psi = xf(\eta), \theta = \theta(\eta), \phi = \phi(\eta) \tag{21}$$

Substituting Eq. (21) into Eqs. (12)–(14), we finally obtain the following system of nonlinear ordinary differential equations:

$$[1+\zeta(1-\theta)]f''' + (f - \zeta\theta')f'' - \left[M^2 + K\left(1+\zeta(1-\theta)\right)\right](f'-1) + 1 - f'^2 = 0 \tag{22}$$

$$\left(1 + \varepsilon\theta + \frac{4R}{3}\right)\theta'' + \Pr f\theta' + \varepsilon\theta'^2 = 0 \tag{23}$$

$$\phi'' + Scf\phi' - Kr\phi = 0 \tag{24}$$

where prime denotes differentiation with respect to η. The respective boundary conditions become

$$\left.\begin{aligned} &f'(0) = 0,\ f(0) = f_w,\ \theta(0) = \frac{1+\lambda\theta'(0)}{1-\lambda\varepsilon\theta'(0)},\ \phi = 1 \ \text{ at } \ \eta = 0 \\ &f' \to 1,\ \theta \to 0,\ \phi \to 0 \quad \text{as} \ \ \eta \to \infty \end{aligned}\right\} \tag{25}$$

2.4. Physical quantities of interest

The quantities of physical interest in this problem are skin friction factor C_f, Nusselt number Nu, and Sherwood number Sh, which are defined, respectively, as follows:

$$C_f = \frac{\mu}{\rho u_e^2}\left(\frac{\partial u}{\partial y}\right)_{y=0} = \mathrm{Re}^{\frac{1}{2}}\left[1+\zeta\left(1-\theta(0)\right)\right]f''(0) \tag{26}$$

$$Nu = -\frac{x}{T_w - T_\infty}\left(\frac{\partial T}{\partial y}\right)_{y=0} = -R\,\mathrm{e}^{\frac{1}{2}}\left(1+\varepsilon\theta(0)+R\right)\theta'(0) \tag{27}$$

$$Sh = -\frac{x}{C_w - C_\infty}\left(\frac{\partial C}{\partial y}\right)_{y=0} = -\mathrm{Re}^{\frac{1}{2}}\phi'(0) \tag{28}$$

Thus, the reduced skin friction factor, reduced Nusselt number Nur, and reduced Sherwood number Shr can be written, respectively, as follows:

$$C_f r = \mathrm{Re}^{-\frac{1}{2}} C_f = \left[1+\zeta\left(1-\theta(0)\right)\right] f''(0) \tag{29}$$

$$Nur = \mathrm{Re}^{-\frac{1}{2}} Nu = -\left(1+\varepsilon\theta(0)+R\right)\theta'(0) \tag{30}$$

$$Shr = \mathrm{Re}^{-\frac{1}{2}} Sh = -\phi'(0) \tag{31}$$

2.5. Particular case

In the absence of a porous medium, i.e., K = 0, and chemical reaction, i.e., K_r = 0, Eqs. (22) and (24) reduce to Eqs. (23) and (25) of Hamad et al. [20]. The constant surface temperature results can be recovered by using small values of λ, i.e., $\lambda \to 0$ in the third boundary condition in Eq.(25) which then gives the condition $\theta(0)$ = 1 (isothermal condition), the same as the third boundary condition in Eq.(27) of Kandasamy and Muhaimin [18] .

Table 1. Comparison of the $f'(\eta)$ and $f''(\eta)$ values for various η values

η	Rahman and Eltayeb [21]		Present results	
	f '(η)	f ''(η)	f '(η)	f ''(η)
0.0	0.0000000000	0.4696000799	0.0000000	0.4696000
0.8	0.3719632881	0.4511900733	0.3719632	0.4511900
1.6	0.6966995257	0.3424871311	0.6966971	0.3424871
2.0	0.8166947347	0.2556691767	0.8166946	0.2556690
3.0	0.9690545877	0.0677102888	0.9690545	0.0677103
5.0	0.9999358634	0.0002578008	0.9999356	0.0002578

3. Numerical Method for Solutions

Since the transformed differential equations are nonlinear, a numerical approach would be more suitable. The system of equations (22)–(24) with boundary conditions (25) are solved numerically by employing a fourth-order Runge–Kutta method and Shooting techniques with a systematic guessing of $f''(0)$, $\theta'(0)$, and $\phi'(0)$.The procedure is repeated until a desired degree of accuracy, namely, 10^{-5} is obtained. The code is written in MATHEMATICA package.

3.1. Code verification

To check the validity of the present code, the $f'(\eta)$ and $f''(\eta)$ values are calculated for $\zeta = \varepsilon = M = K = f_w = 0$ and for different η values. Note that this is for the case of the Falkner–Skan boundary layer equation with wedge angle parameter $\beta = 0$. From Table 1, it is found that the data produced by the present code and those of Rahman and Eltayeb [21] are in excellent agreement; thus, the use of the present numerical code for the current model is justified.

4. Numerical Results and Discussion

To provide a physical insight into the study, complete numerical calculations are carried out using the method described in the previous section for various values of chemical reaction parameter K_r, permeability parameter K, surface convection parameter λ, viscosity parameter ζ, suction parameter f_w, and thermal conductivity parameter ε. In the simulation, the default values of the parameters are assumed to be Pr = 0.71, M = 0.5, ζ =2.0, f_w = 0.4, K = 2, ε = 0.1, λ = 0.2, K_r = 0.5, and R = 0.3 unless otherwise indicated.

Table 2. Effects of K, f_w, and R on $C_f r$,Nur, and Shr

K	f_w	R	$C_f r$	Nur	Shr
0.0	0.2	0.3	2.03818	0.667431	-
1.0			2.54219	0.653941	-
2.0			2.93398	0.634092	-
	0.0		2.00976	0.581681	0.701842
	0.4		2.31022	0.714408	0.929598
	0.8		2.62529	0.854578	1.187550
	0.2	0.0	-	0.563312	-
		0.3	-	0.646896	-
		0.6	-	0.733695	-

Table 2 shows that an increase in permeability parameter K leads to an increase in the skin friction. Thus, the permeability parameter imposes an additional shear stress on the boundary. In addition, the skin friction factor increases with increasing values of surface convection parameter λ and viscosity parameter ζ. The heat transfer rate at the plate increases with increasing f_w and ε values, as shown in Tables 2 and 3.On the other hand, the rate of heat transfer decreases with an increase in surface convection parameter λ and permeability parameter K. It is evident that the effect of viscosity parameter ζ on the heat transfer rate is insignificant. Table 2 also shows that suction parameter f_w leads to an increase in the rate of mass transfer. It is observed from Table 3 that an increase in the chemical reaction parameter K_r leads to an increase in the Sherwood number for destructive reaction; this finding is consistent with the result of Kandasamy et al. [23]. However, an increase in the chemical reaction parameter for generative reaction leads to a decrease in the Sherwood number. Furthermore, it is worth noticing from Table 3 that the numerical value of Sherwood number is higher in the case of a destructive reaction than in the case of a generative reaction.

Table 3. Effects of λ, ε, ζ, and K_r on C_fr, Nur, and Shr

λ	ε	ζ	Kr	C_fr	Nur	Shr
0.0	0.1	2.0	0.4	2.13271	0.822491	-
0.2				2.31022	0.721242	-
0.4				2.44138	0.644114	-
0.1	0.0			-	0.751887	-
	0.1			-	0.768096	-
	0.2			-	0.783802	-
	0.1	1.0		2.06551	0.768718	-
		3.0		2.55226	0.767792	-
		5.0		3.03202	0.767623	-
		2.0	0.0	-	-	0.825004
			0.4	-	-	1.047000
			0.8	-	-	1.234281
			-0.2	-	-	0.694844
			-0.4	-	-	0.546236

We now discuss the graphical results, which provide an additional insight into the problem under study.

4.1. Computational results for velocity profiles

Figure 2 illustrates the variation in the velocity distributions across the boundary layer for various values of permeability parameter K. It is evident from the figure that the increasing values of permeability parameter enable the fluid to flow at a slower rate, which is minimal near the boundary region. Thus, an increase in *K* reduces the momentum boundary layer thickness. As the porosity of the medium increases, the *K* value decreases. For large porosity of the medium, i.e., for decreasing *K*, the fluid gets more space to flow and, as a consequence, its velocity increases. It is worthy mentioning that these profiles satisfy the far field boundary conditions. The effect of suction parameter f_w on the velocity distribution for a permeable plate is shown in Fig. 3 in the absence and presence of a porous medium. It is observed from the figure that the velocity distribution across the boundary layer increases with an increase in suction parameter f_w in both cases, i.e., for $K = 0$ and $K = 1$. The variations in the velocity profiles against transverse coordinate η are shown in Fig. 4 for various values of viscosity parameter ζ. It is evident that the velocity profiles decrease within the boundary region for both $K = 1$ and $K = 0$ with an increase in the ζ values; accordingly, the momentum boundary layer thickness decreases. It should be noted that the effect of ζ is apparent in presence of a porous medium. Thus, the effect of the permeability parameter is dominant over that of the viscosity variation parameter.

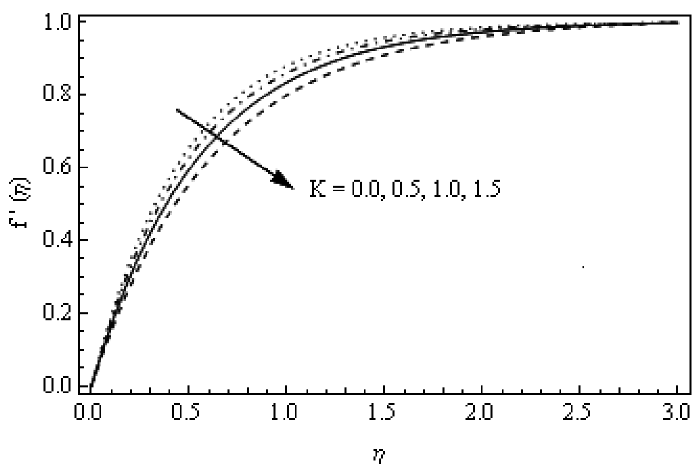

Fig. 2. Velocity profiles for various *K* values.

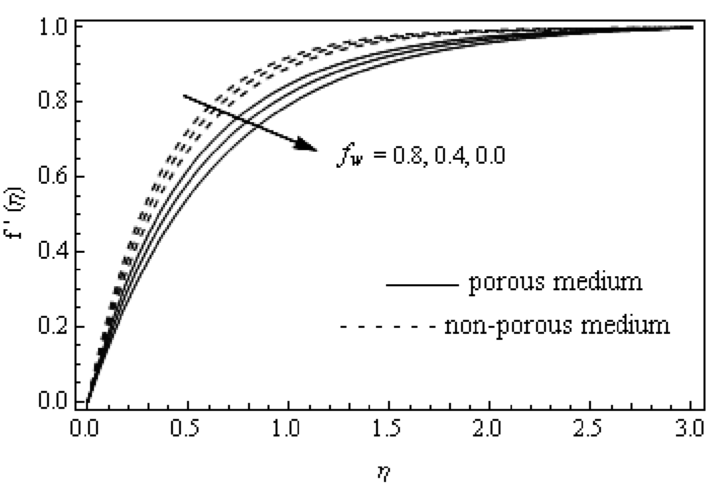

Fig. 3. Velocity profiles for various f_w values.

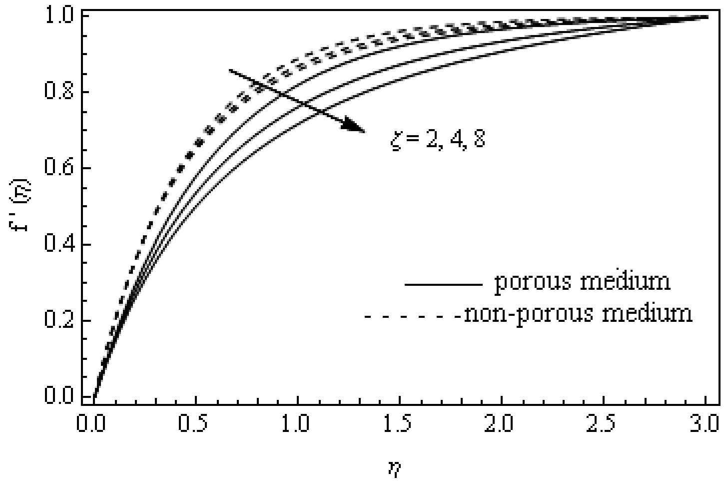

Fig. 4. Velocity profiles for various ζ values.

4.2. Computational results for temperature profiles

The effect of permeability parameter K on the temperature distribution is revealed in Fig. 5; it is observed that an increase in the K values results in an increase in fluid temperature in the boundary layer region. The effect of increasing K values opposes the flow in the boundary layer region. This finding is attributed to the fact that the presence of a porous medium resists the fluid motion; as a result, more heat is transferred from the sheet to the fluid. Thus, the temperature rises in the boundary layer region in the presence of a porous medium.

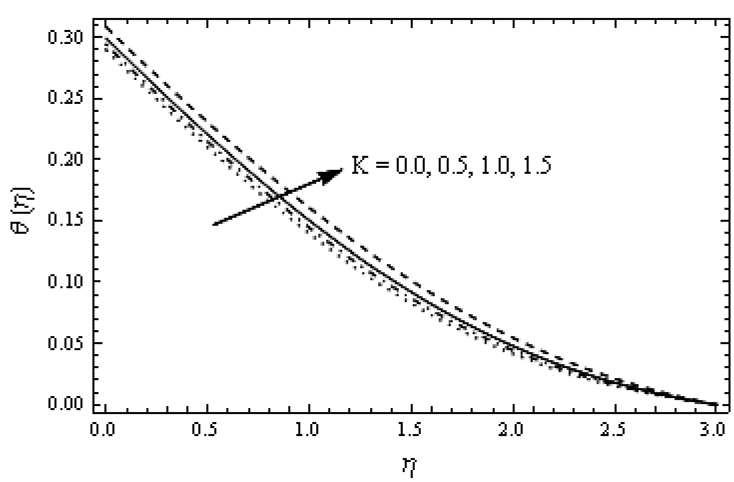

Fig. 5. Temperature profiles for various K values.

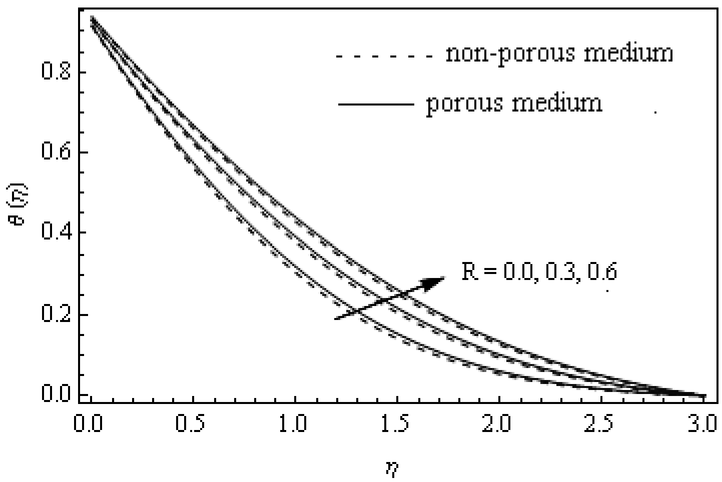

Fig. 6. Temperature profiles for various *R* values.

The impact of thermal radiation parameter *R* on the temperature profiles is shown in Fig. 6. For a nonzero fixed value of η, temperature distribution across the boundary layer increases with increasing *R* values; therefore, the thermal boundary layer thickness increases.

It is evident from Fig. 7 that the effect of suction parameter f_w on the temperature profiles is noticeable only in a region close to the sheet. It can easily be seen from the figure that the temperature distribution across the boundary layer decreases with increasing f_w values for suction in the presence and absence of a porous medium; therefore, the thermal boundary layer thickness decreases.

Figure 8 shows that the temperature decreases rapidly as η increases and there is a significant increase in the rate of increase in temperature with an increase in thermal conductivity parameter ε .

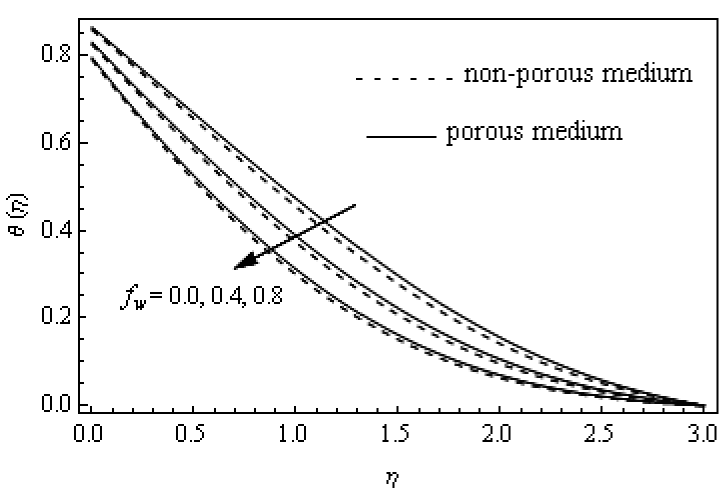

Fig. 7. Temperature profiles for various f_w values.

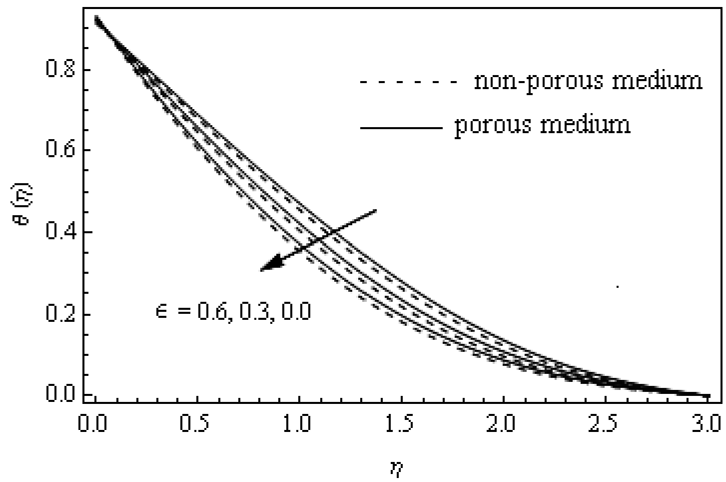

Fig. 8. Temperature profiles for various ε values.

Figure 9 shows the effects of surface convection parameter λ on fluid temperature in the presence/absence of a porous medium.

It is observed from the figure that temperature $\theta(\eta)$ decreases with increasing λ in the boundary layer region and attains a maximum value at the surface of the plate. The result tends to the solution for a constant surface temperature for small λ values, i.e., $\lambda \to 0$. From boundary condition (25), it is evident that θ (0) =1 as $\lambda \to 0$. Again, these observations show good agreement with the results of Hamad et al. [20].

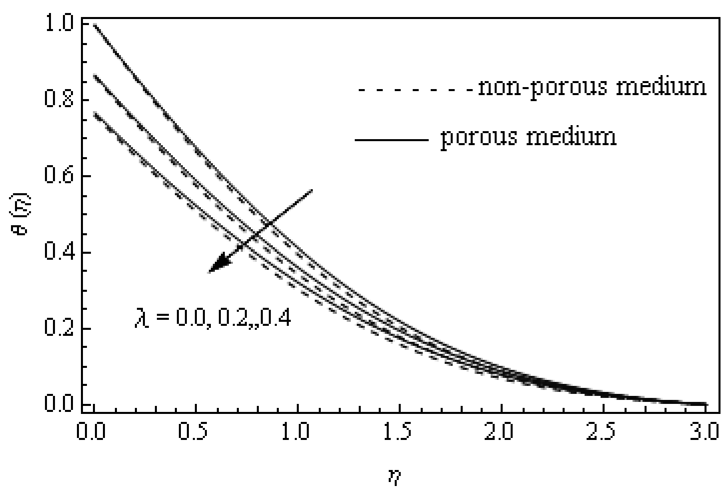

Fig. 9. Temperature profiles for various λ values.

The effect of viscosity parameter ζ on temperature distribution in the presence/absence of a porous medium is shown in Fig. 10. It is seen that the thermal boundary layer thickness increases as ζ increases with a consequent enhancement of the temperature in the boundary layer region.

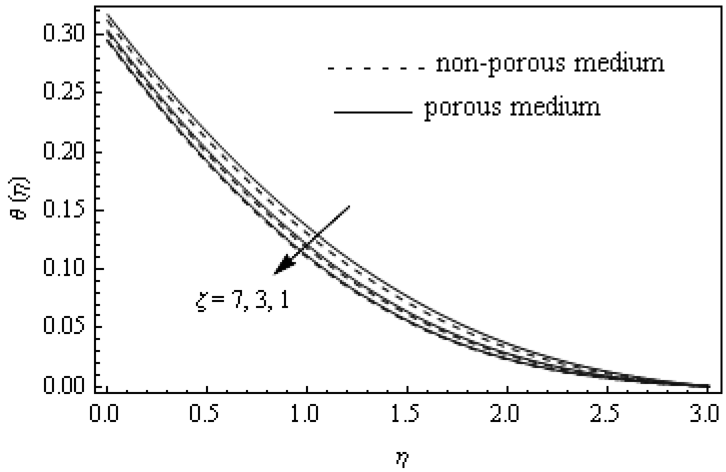

Fig. 10. Temperature profiles for various ζ values.

4.3. Computational results for concentration profiles

Figure 11 shows the concentration profiles against η for several values of chemical reaction parameter K_r (>0) in the presence of wall suction. An increase in chemical reaction parameter K_r (>0) leads a decrease in the concentration of the conducting fluid along the wall of the surface as shown in Fig. 11. Therefore, in the case of a destructive reaction, the chemical reaction parameter decelerates the concentration of the fluid across the boundary layer; as a consequence, the concentration boundary layer becomes thin for larger chemical reaction parameter K_r. In particular, the concentration of the fluid gradually changes from a higher value to a lower value only when the strength of the rate of chemical reaction K_r is higher than kinematic viscosity ν of the fluid.

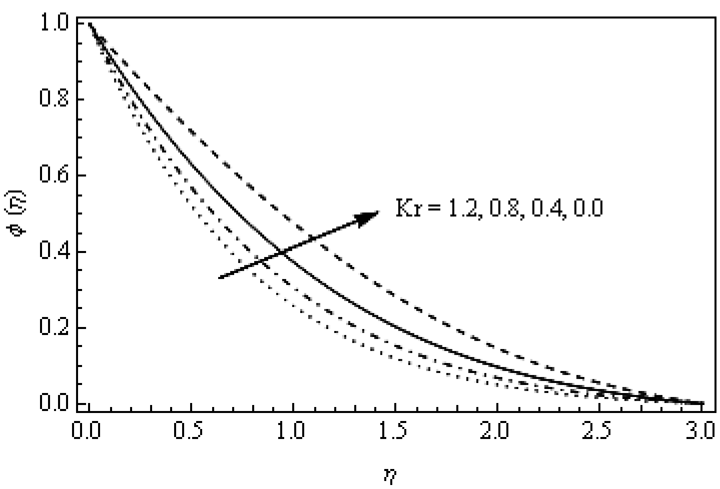

Fig. 11. Concentration profiles for various K_r values (>0).

The variation in the concentration distribution across the boundary layer for different values of chemical reaction parameter K_r (<0) is shown in Fig. 12. It is clear from the figure that the concentration increases tremendously in the presence of generative reaction of the chemical reaction. It is worth mentioning that the effect of generative reaction on the concentration profiles is much more pronounced than that of the destructive reaction, as shown in Fig. 12.

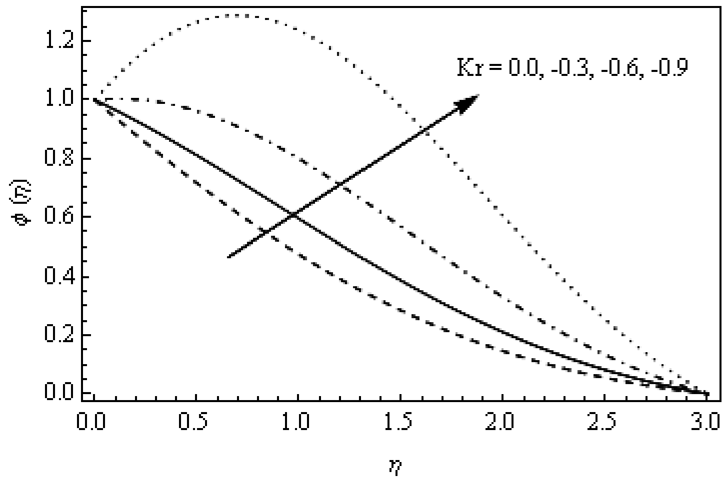

Fig. 12. Concentration profiles for various K_r values (<0).

Figure 13 illustrates the effect of suction parameter f_w on the concentration distribution. It is evident that an increase in the values of suction parameter f_w results in a decrease in the concentration distribution in the boundary layer region.

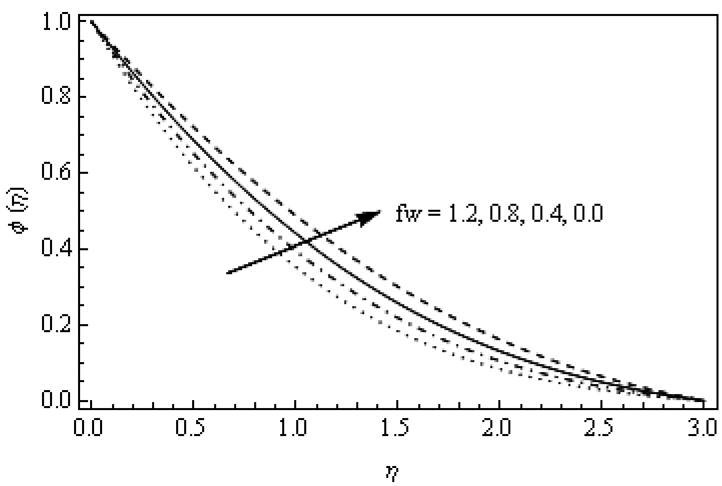

Fig. 13. Concentration profiles for various f_w values.

5. Conclusions

Using scaling group transformations, the similarity solutions of a MHD forced convective flow of an electrically conducting incompressible fluid over a permeable flat plate embedded in a porous medium with thermal convective surface boundary conditions have been obtained to study the effect of thermal radiation, temperature-dependent viscosity and thermal conductivity in the presence of a first-order chemical reaction. The main outcomes of the study are listed below:

- The effect of the porosity parameter on an electrically conducting incompressible fluid is to suppress the fluid velocity which, in turn, causes an enhancement in the temperature field.

- In the forced convection regime, the imposition of wall fluid suction increases the entire hydrodynamic boundary layer and reduces the thermal and concentration boundary layers causing the fluid velocity to rise, while decreasing its temperature and concentration.

- For a first-order chemical reaction, the concentration decreases with increasing chemical reaction parameter for a destructive reaction, whereas the effect is reversed for a generative reaction.

- The effect of permeability parameter is to decrease the rate of heat transfer. This result has significant industrial applications where the power expenditure can be minimized by increasing the porosity of the permeable plate.

References

[1] A. G. Hansen, Similarity Analysis of Boundary Layer Problems in Engineering, Prentice Hall, Englewood Clis, New Jersey, 1964.
[2] W. F. Ames, Nonlinear Partial Differential Equations in Engineering, Academic Press, New York, 1972.
[3] M. Yurusoy and M. Pakdemirli, Int. J. Eng. Sci. 35, 731, (1997).
[4] M. Yurusoy, M. Pakdemirli, and O.F. Noyan, Int. J. Nonlinear Mech. 36, 955, (2001).
[5] M. L. Gandarias, M. Torrisi, and R. Tracina, J. Phys A: Math. Theor. 40, 8803, (2007).
[6] N. Pandey, B.D. Pandey, and V.D. Sharma, Appl. Math. Comput. 215, 681, (2009).
[7] G. C. Layek, S. Mukhopadhyay, and Sk. A. Samad, Int. Commun. Heat Mass Transfer 34, 347, (2007).
[8] K. Hiemenz. Dingl. Poltech. J. 32, 321, (1911).
[9] R. Tsai and J.S. Huang, Int. J. Heat Mass Transfer 52, 2399, (2009).
[10] A. Aziz, Commun. Nonlinear Sci. Numer. Simul. 14, 1064, (2009).
[11] G. M. Abdel-Rahman, Physica B 405, 2560, (2010).
[12] A. J. Chamkha and Abdul-Rahim A Khaled, Int. J. Numer. Methods Heat Fluid Flow 10, 94, (2000).
[13] M. A. Seddeek, A. A. Darwish, and M. S. Abdelmeguid, Commun. Nonlinear Sci. Numer. Simul. 12, 195, (2007).
[14] M. Pakdemirli and M. Yurusoy, Soc. Ind. Appl. Math. Rev. 40, 96, (1998).
[15] M. Yurusoy and M. Pakdemirli, Mech. Res. Comm. 26, 171, (1999).
[16] M. Oberlack, J. Fluid Mech. 379, 1, (1999).
[17] M. A. Seddeek and A.M. Salem, Heat Mass Transfer 41, 1048, (2005).

[18] R. Kandasamy and I Muhaimin, Transp. Porous Media 84, 549, (2010).
[19] S. Mukhopadhyay and G.C. Layek, Meccanica 47, 863, (2012).
[20] M. A. A. Hamad, Md.J. Uddin, and A.I.Md. Ismail, Nucl. Eng. Des. 242, 194, (2012).
[21] M. M. Rahman and I.A. Eltayeb, Int. J. Therm. Sci. 50, 468, (2011).
[22] P. M. Patil and P.S. Kulkarni, Int. J. Therm. Sci. 47, 1043, (2008).
[23] R. Kandasamy, I. Muhaimin, and H. B. Saim, Nucl. Eng. Des. 240, 39, (2010).
[24] R. Kandasamy, I. Muhaimin, and H. B. Saim, Commun Nonlinear Sci. Numer. Simul. 15, 2109, (2010).
[25] R. Kandasamya, T. Hayat, and S. Obaidatc, Nucl. Eng. Des. 241, 2155, (2011).
[26] M. H. Yazdi, S. Abdullah, I. Hashim, and K. Sopian, Int. J. Heat Mass Transfer 54, 3214, (2011).
[27] W. M. Kays and M. E. Crawford, Convective Heat and Mass Transfer, 4th ed., McGraw Hill, New York, 2005.
[28] T. C. Chiam, Acta Mech. 129, 63, (1998).
[29] T. A. Savvas, N. C. Markatos, and C. D. Papaspyrides, Appl. Math. Model. 18, 14, (1994).